The Strait of Gibraltar

Overview

The Strait of Gibraltar is located between the southern coast of Spain and the northern coast of Morocco (35°45' to 36°10' N. latitude and 5°10' to 6°00' W. longitude). It is the single connection between the Atlantic Ocean and the Mediterranean Sea. Water flow through the straight consists of an upper layer of Atlantic water flowing eastward over a lower layer of Mediterranean water flowing westward. (Figure 3)

The strait has been an area of intense study in order to understand and characterize this exchange of water of between the Atlantic and Mediterranean. Early studies are described in Defant [1961], while Lancombe and Richez [1982] describe an investigation carried out in the 1960's over several ocean campaigns under the aegis of the NATO subcommittee on Oceanographic Research. Those data were also used by Armi and Farmer [1985] to interpret the hydraulic flow through the Straight and helped motivate the Gibraltar Experiment carried out in 1985-1986 [La Violette et al. 1986; Kinder and Bryden 1987, Armi and Farmer, Farmer and Armi 1988]. Armi and Farmer used data collected as part of that experiment to examine the details of the flow within the strait, identifying a number of hydraulic control points at the Tarifa Narrows, the Camarinal Sill, the Spartel Sill and at a location west of the Spartel Sill. A comprehensive atlas of the hydrology and currents can be found in [Landcombe and Richez 1984]

Internal waves are an important feature in the strait. During most tidal cycles, eastward propagating internal waves are generated through the interaction of the flow with the Camarinal Sill. The waves are released about the time of high water and propagate eastward along the strait as an internal bore [Armi & Farmer 1988, Farmer and Armi 1988]. The density difference between the Atlantic and Mediterranean waters, due primarily to their salinity differences, provides the necessary stratification. Observations of internal waves have been made since the 1930's. Data have been collected in-situ (CTD, Acoustic Doppler Current Profilers), by ship radar, shore based radar, airborne SAR, orbital SAR, aerial photography and astronaut photography. [See Frassetto, 1960; Ziegenbein 1969; Boyce, 1975; Lacombe and Richez, 1982; La Violette et al. 1986; Armi and Farmer 1988; Bray et al. 1990, Pettigrew and Hyde 1990; Watson and Robertson 1990, Alpers and La Violette 1992, Richez, 1994, Brandt et al. 1996; Alpers et al. 1996, Apel, 2000, Apel and Worcester 2000] The list is by no means exhaustive.

Orbital SAR imagery and astronaut photography since the late 1980's have provided a synoptic view of the internal waves in Gibraltar. The imagery revealed a complex pattern of internal wave patterns and interactions. Four major patterns have emerged from the data.
1) Internal waves produced by the tidal interaction with the Camarinal Sill that propagate eastward out into the Mediterranean and Alboran Sea.
2) Internal waves produced at the Camarinal Sill that propagate westward into the Atlantic. These waves are weaker then the eastward propagating waves and are present much less often.

3) Internal waves, of unknown origin, propagating north and south between Gibraltar and Ceuta at the eastern edge of the strait.
4) A standing surface roughness pattern over the Camarinal Sill. This is thought to be the surface manifestation of quasi-stationary depression of the stratification in the region [Brandt et al. 1996]

Table 1 presents a summary of the characteristics of the internal wave that propagate eastward from the Strait of Gibraltar. The values have been reported in the literature and derived from both in-situ and remote sensing data sources. Table 2 shows the months during the year when these internal waves have been observed. It is believed that the waves occur year round and that the November and December gap would be eliminated with the examination of more imagery.

Table 1. Characteristic Scales for Strait of Gibraltar

Packet Length L (km)	Along Crest Length C_r (km)	Maximum Wavelength λ_{MAX} (km)	Internal Packet Distance D (km)
3 - 20	15 - 100	1000 - 3000	25 - 30
Amplitude $2h_0$ (m)	Long Wave Speed c_0 (m/s)	Wave Period (min)	Surface Width l_1(m)
-50 to -80	1 - 2	5 - 19	1 – 1.5

Table 2 - Months when eastward Propagating Internal Waves have been observed At the Strait Of Gibraltar

Jan	Feb	Mar	Apr	May	Jun	Jul	Aug	Sept	Oct	Nov	Dec
X	X	X	X	X	X	X	X	X	X		

Eastward Propagating Internal Waves

Generation

Solitons radiating eastward from the Strait of Gibraltar are formed by an intense westward tidal flow across the Camarinal Sill. Strong tidal flow over the sill regularly produces solitons with amplitudes of 50 to 100 m and wavelengths of two to four km [Farmer and Armi; Armi and Farmer, 1988]. Figure 1 presents the overall bathymetry and key features of the strait. A cross sectional profile of the prominent features along the strait produced by echo-sounder is shown on Fig. 2 [Armi and Farmer, 1988; Farmer and Armi, 1988]. The stratification in the strait, necessary for internal wave production, is provided by the salinity difference between the lower salinity, upper layer Atlantic water flowing east and higher salinity lower Mediterranean water flowing west (Figure 3).

Internal waves in the area begin with a steep depression in the pycnocline at the sill. The lee wave structure that forms is the internal response to a strong eastward flow over the sill [Armi & Farmer 1988, Farmer and Armi 1988]. Figure 5 shows an isopycnal σ_θ = 28.0 kg/m^3 plunge over 100 m at 4.3 h at which time there is the onset of the undulatory bore. The bore quickly forms a sequence of solitary waves at its leading edge. Figure 5 shows approximately five oscillations. A several-hour depression of the thermocline with an amplitude of approximately one-half that of the lead soliton exists to the rear of the packet. Over the remainder of the tidal period, the

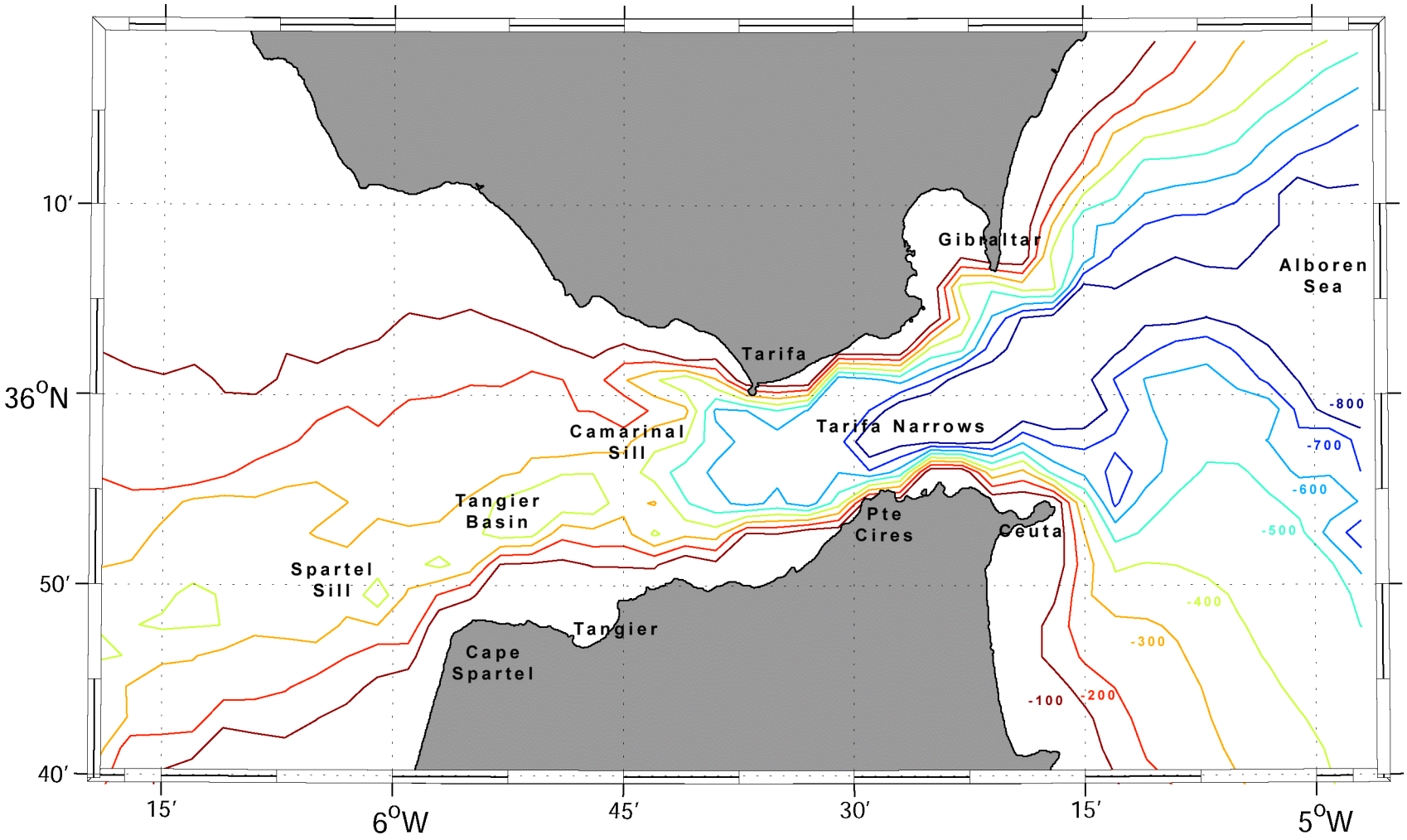

Figure 1: Bathymetry map of Gibraltar (Derived from Smith and Sandwell version 8.2)

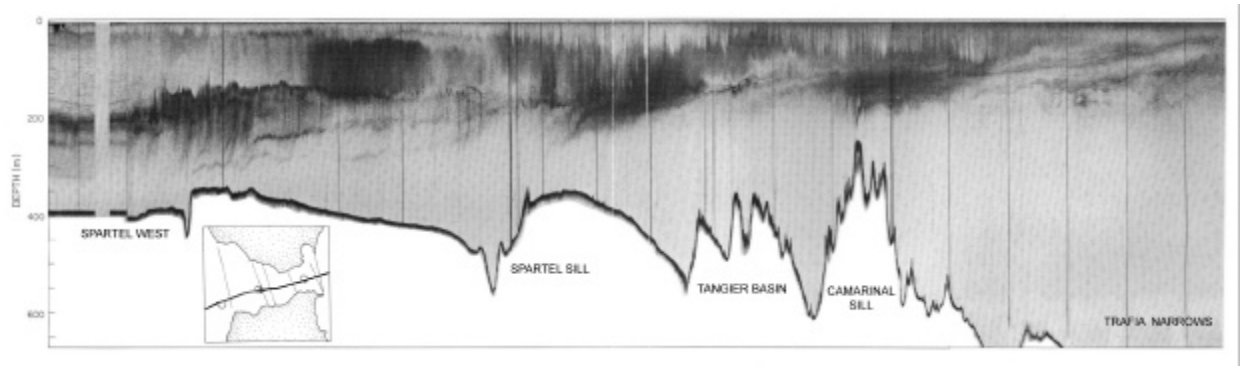

Figure 2. Transect of the Strait [From Armi and Farmer, Farmer and Armi.1988]

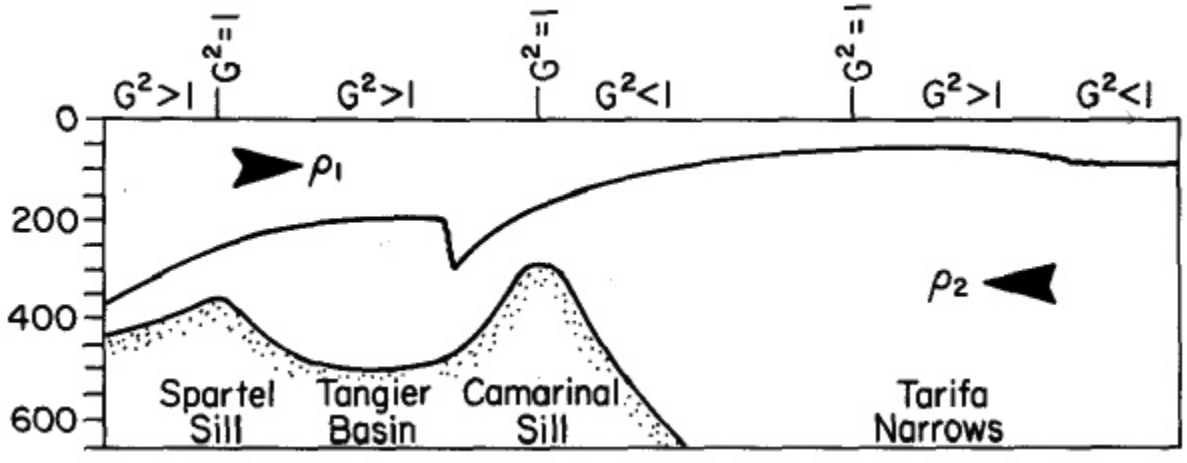

Figure 3, Simplified drawing showing a hypothetical steady state representation of the interface position in the Strait of Gibraltar with major topographic features. [From Armi and Farmer, Farmer and Armi.1988]

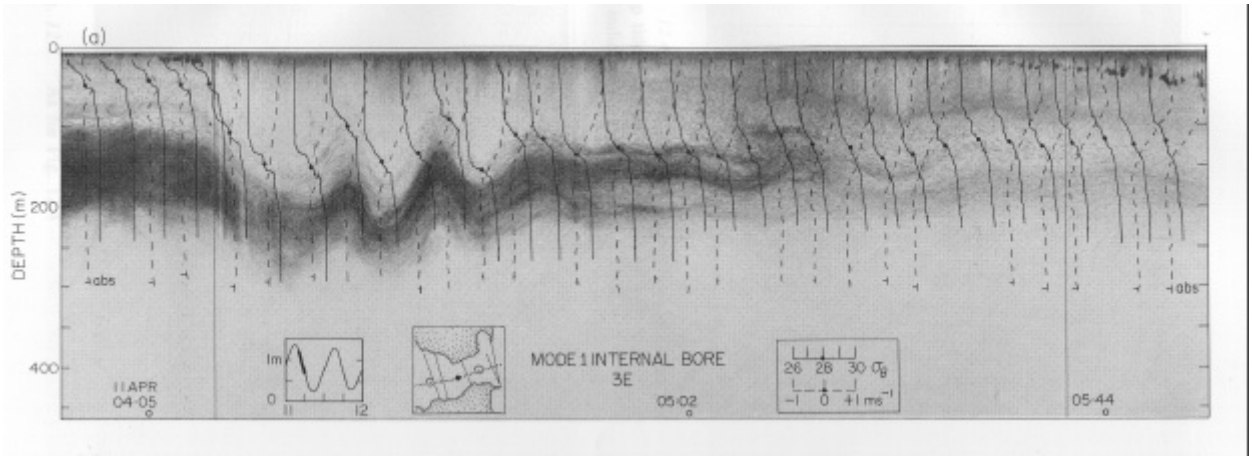

Figure 4. Echo-sounder profile of large soliton packet in the center of Tarifa Narrows in Gibraltar, taken in April 1986. The lead (leftmost) soliton shows considerable broadening, possibly due to higher-order nonlinearities at work there. Double amplitude $2h \approx 80$ m. Solid vertical lines are densities from CTD casts, and dashed lines are relative east-west velocity profiles from ADCP's. [From Armi and Farmer, Farmer and Armi.1988]

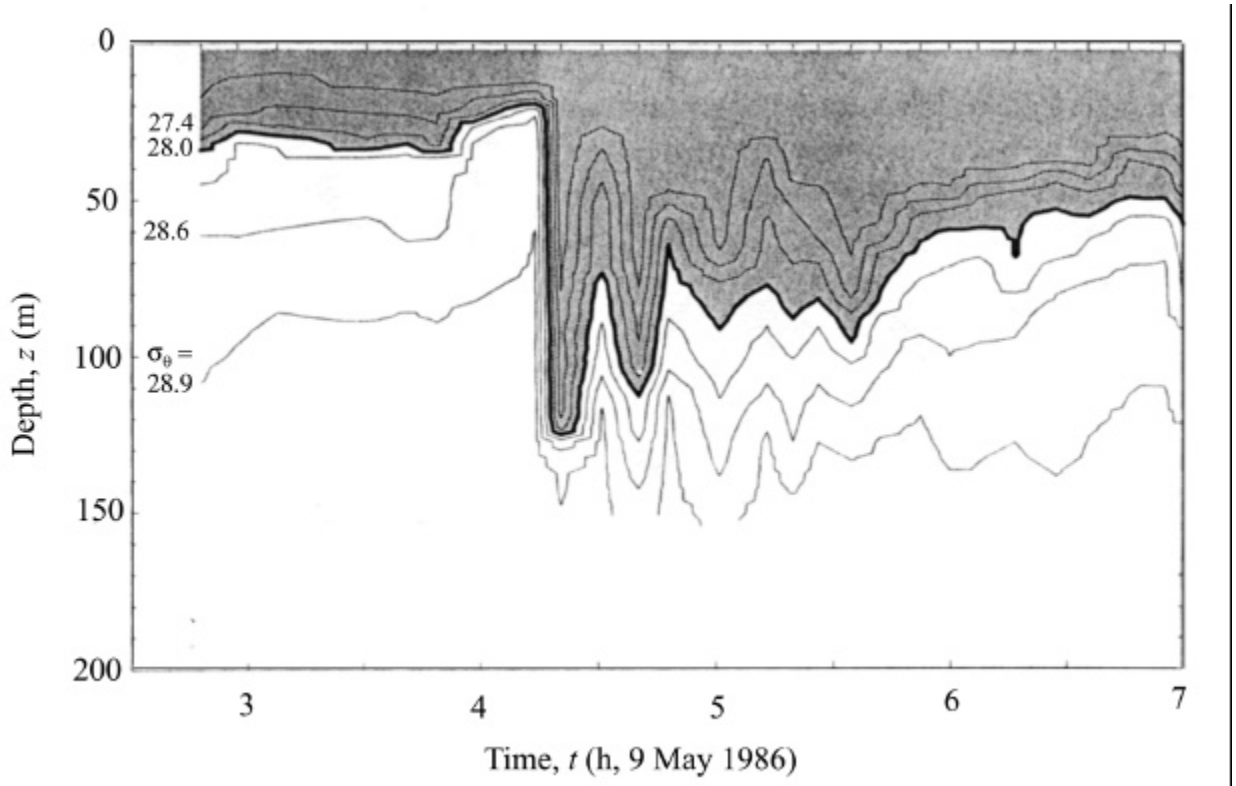

Figure 5 Lee wave observed in the Tarifa Narrows Strait of Gibraltar via Advanced Microstructure Profiler. The isopycnal σ_θ = 28.9 psu plunges by over 100 m at about 4.2 h, and is followed by a longer-term pycnocline depression. Upper level currents ≤ 0.6 m/s to the east; lower level currents ≤ 0.4 m/s to the west. Data courtesy Wesson and Gregg [1987]

system recovers to quasi-equilibrium or perhaps more accurately, to a quiescent state of internal displacements. The entire 12-½ h cycle constitutes the internal baroclinic tide in the region. Figure 4 shows an echo sounder profile of the internal bore as it travels east in the Tarifa Narrows. The visible bore is characterized by two to three large internal waves followed by a less orderly interfacial disturbance. [Armi & Farmer 1988, Farmer and Armi 1988]

Imagery

Figures 6 - 9 are ERS SAR images that represent the progress of four wave packets from their origin near the Camarinal Sill west of Gibraltar to over 200 km into the Alboran Sea. All four were taken in spring or early summer. These data show features that are consonant with nonlinear soliton characteristics moving in current systems: (a) amplitudes depend on tidal current and Froude number, hence the semi-diurnal variations in regions where the tides are mixed semi-diurnal and diurnal; (b) advection by background currents with speeds of the order of tens of cm/s is important when wave phase speeds are close to current speeds; (c) packets spread out from small sources, larger waves outpace smaller waves, and the packet continues to draw apart and spread radially as time goes on.

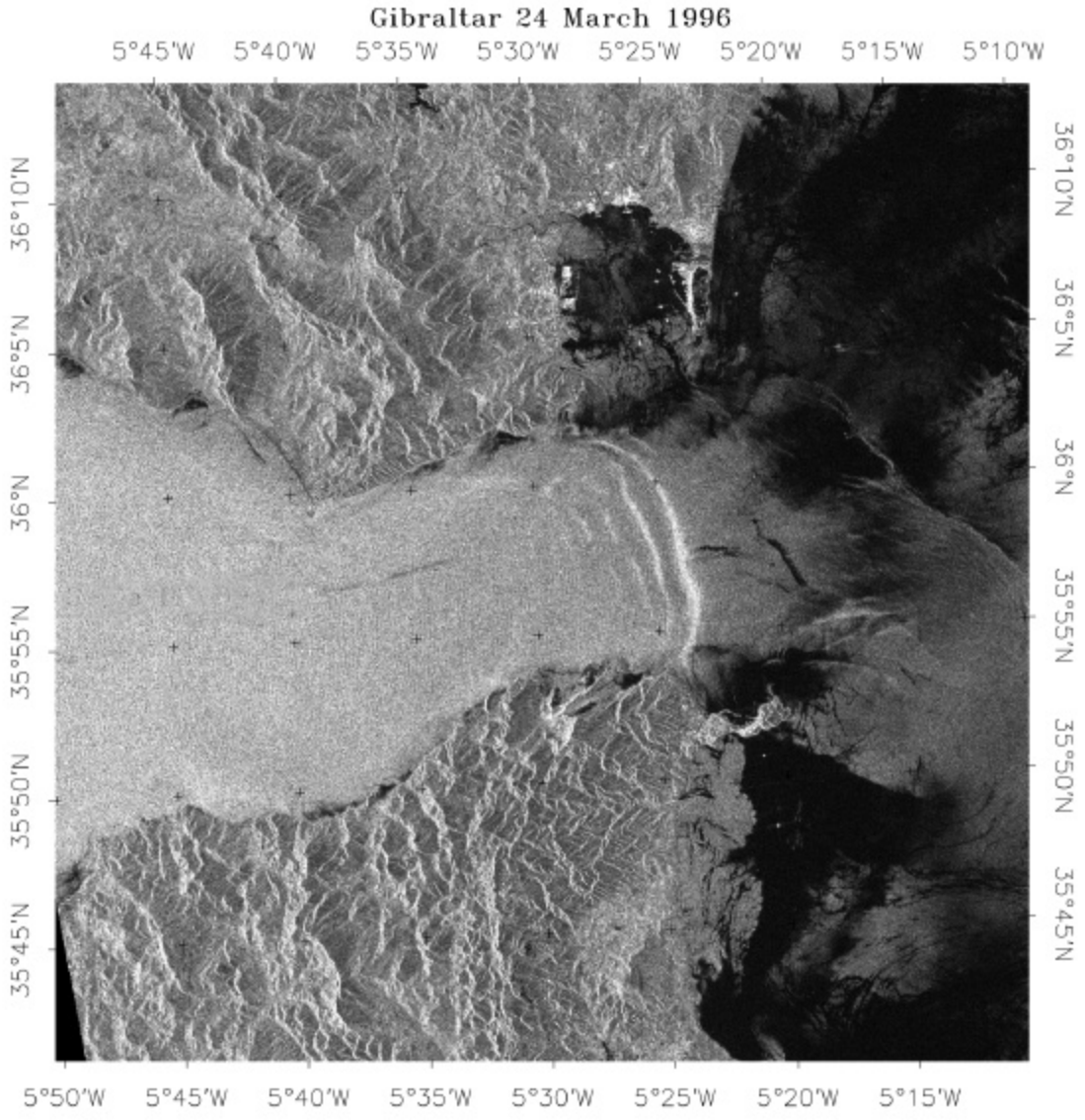

Figure 6. ERS-1 image for March 24, 1996 at 22:39:24, showing a newly formed soliton packet propagating through the Strait of Gibraltar. Five oscillations are visible. The lead crest is approximately 30 km from the generation point at the Camarinal Sill. Original image © Copyright ESA

There appears to be at least two modes of propagation for the eastward waves, the Northeast Mode and the Southeast Mode, named for the tendency of the pulse, on the average, to head in the directions indicated. The waves in the NE Mode propagate toward the south coast of Spain to the Costa del Sol, while the SE mode waves tend toward the north coast of Morocco. There may also be a third mode wherein the main pulse of solitons moves down the middle of the deep Alboran Basin toward Isla de Alborán, a distance of over 200 km from their formative regions. There is also some weak evidence that the solitons may alternate modes on a semidiurnal basis, mainly in those few images capturing more than one pulse.

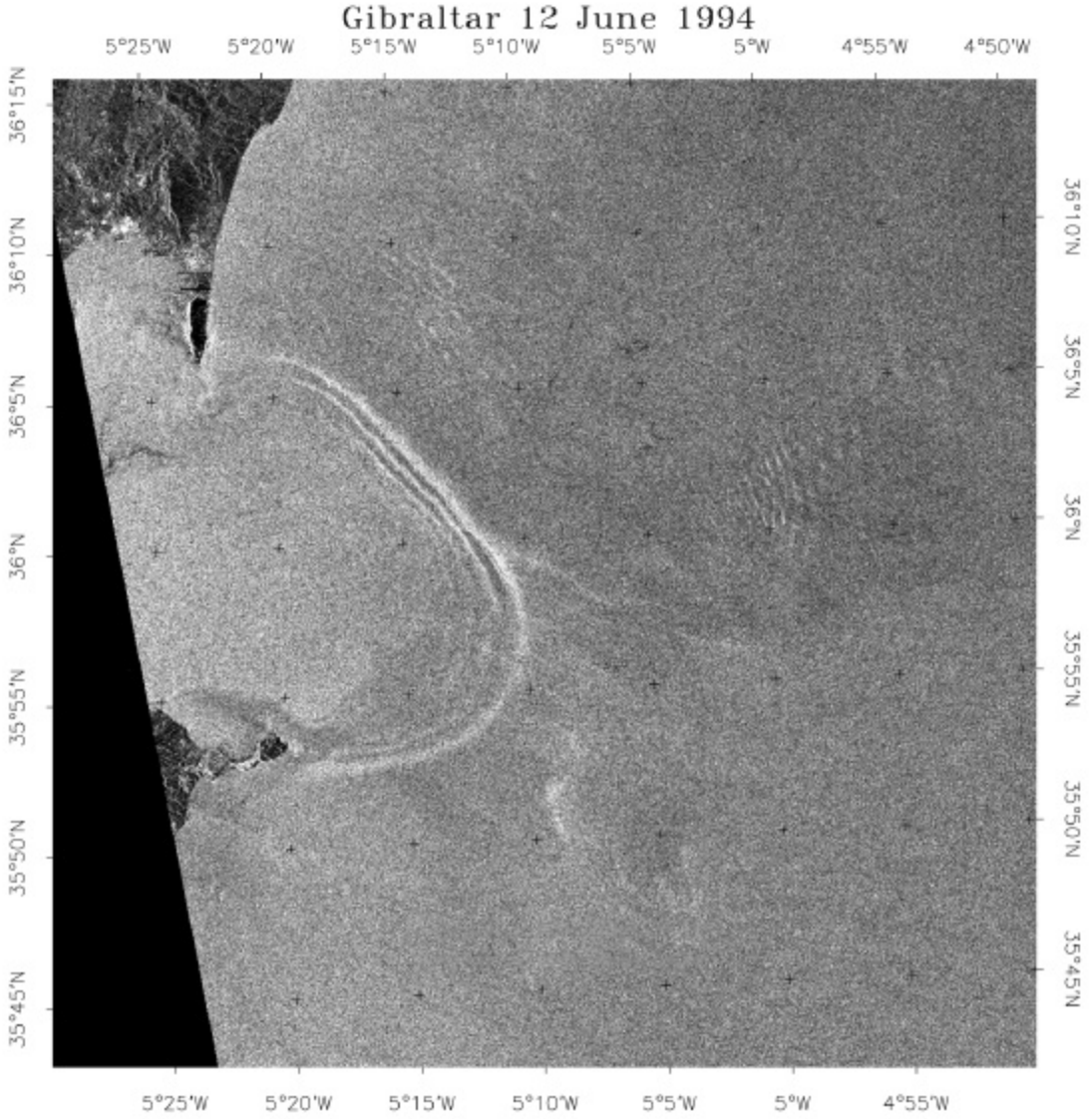

Figure 7. ERS-1 image for June 12, 1994 at 22:37:25. Soliton packet has broken free of Strait of Gibraltar and radiates as a curved wavefront determined by a combination of refraction, diffraction, and tidal advection. It is propagating in the "Southeast Mode." The lead soliton is approximately 55 km from the Camarinal Sill. Original image © Copyright ESA

It is likely that the two (or three) modes observed here are associated with tidal modulation of the Atlantic inflow to the Alboran, since the two basins have differing tidal phases. Variable wind-driven currents are also appreciable here. Since soliton phase speeds are quite similar to upper-ocean current speeds, one expects considerable current-induced wave refraction and even shear-flow amplification/instability. In order to understand the relationship of the soliton propagation to the upper sea currents, much more data are required.

Figure 6 (24 Mar 1996) shows a young wave packet, having reached only to the centerline of Gibraltar Bay. There are four oscillations whose wavelengths are about 1½ km and which are fairly uniform at this stage. Atlantic winds and long surface waves are penetrating into the

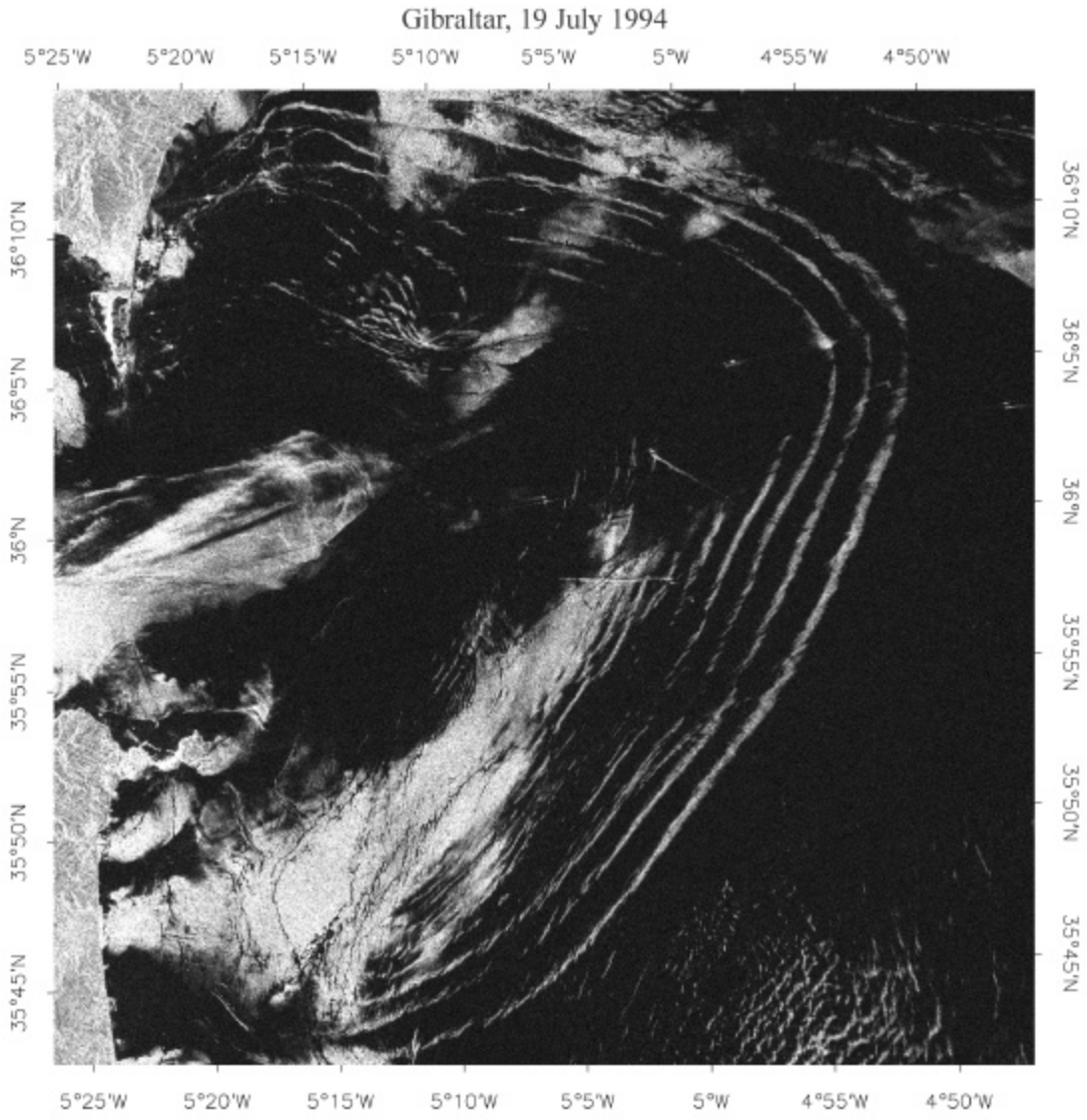

Figure 8. ERS-1 image for July 19, 1994 at 22:38:10. A large packet advances into the Alboran Sea, developing a new oscillation each buoyancy period and diminishing in amplitude as time goes on. The center of the wavefront shows evidence of advection by large-scale current, probably tidal. The lead soliton is approximately 80 km from Camarinal Sill. Original image © Copyright ESA

Alboran Sea about as far as the leading crest, but over much of the right side of the image, winds are light. Several distinct groups of short-wavelength internal waves lie just ahead of the Gibraltar front.

Figure 7 (12 Jun 1994) shows a newly formed soliton packet radiating from the eastern mouth of the Strait, and shows a tendency to refract to the SE. Three or four solitons are in the emerging packet. The signature of the group is quite intense, in spite of what appears to be a strong surface wind field over much of the western Mediterranean. To the east at a distance of roughly 25 km, another weak packet is visible. The differences in intensities between the earlier packet and the present one suggest that a threshold effect may exist, wherein tidal flow must

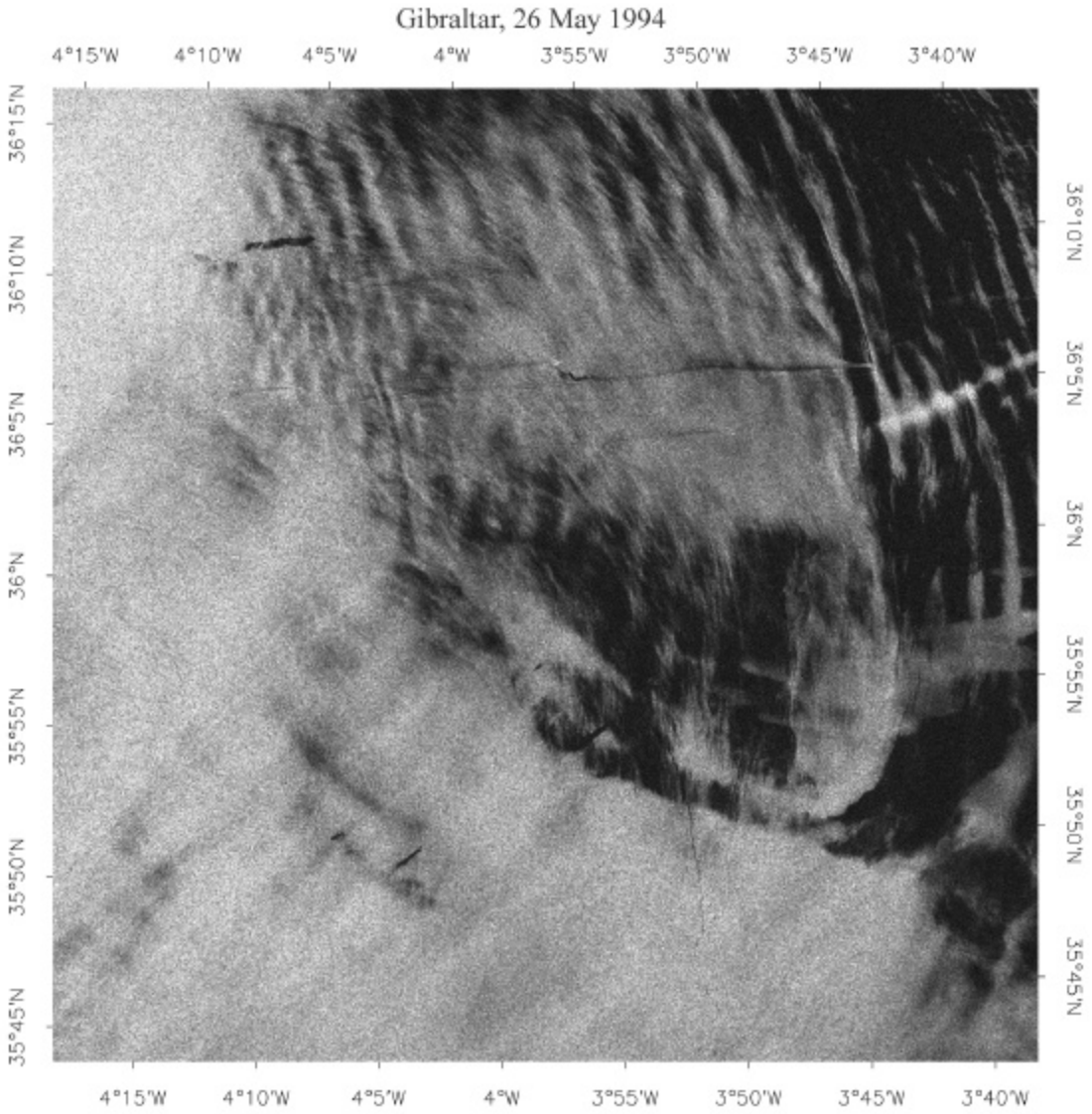

Figure 9. ERS-1 image for May 26, 1994 at 22:34:20. Soliton packet has propagated for some 50 h and has reached over 200 km from formation region and developed over 30 oscillations. Spreading of packet is due to the range of amplitude-dependent phase speeds present. Original image © Copyright ESA

exceed a critical value of Froude number before an internal soliton may develop. Most soliton sites produce their maximum wave heights and numbers near the spring phase of the fortnightly cycle and little or no waves near the neap phase.

Figure 8 (19 Jul 1994) shows an immense soliton packet that has broken free of the mouth of the Strait, apparently radiating in the NE Mode. Upwards of 10 or more solitons are in the emerging packet. Another small packet is just emanating from the mouth. The large packet is propagating at its highest speed in the deep water of the Alboran Basin and may split in two, with refraction bending the two arms through 180° as they approach shore. Residual waves off the east coast of Morocco appear to have been scattered by the submarine canyon, in the south-central part of the image. They were probably formed on the previous tidal cycle in the SE Mode.

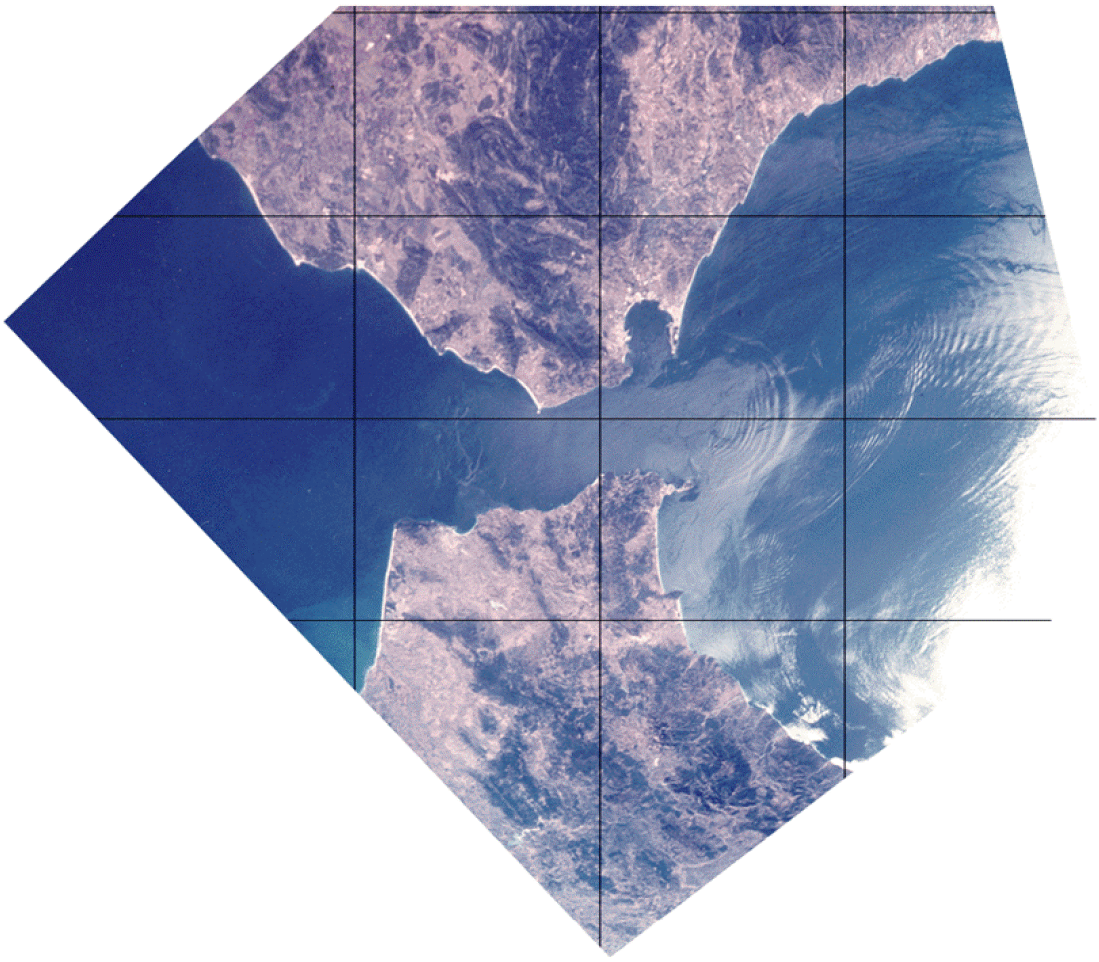

Figure 10. Photo of Gibraltar region from U.S. Space Shuttle, STS-41G, Oct. 11, 1984, orthorectified. Latitude lines are at 20' intervals and longitude lines are at 30' spacings. Three packets of solitons are seen to the east, apparently alternating in the Northeast and Southeast Modes; older packets are visible along Spanish and Moroccan coasts. Original Image (STS41G-34-81) Courtesy of Earth Sciences and Image Analysis Laboratory, NASA Johnson Space Center (http://eol.jsc.nasa.gov)

Figure 9 (26 May 1994) shows a well-evolved soliton packet approaching Isla de Alborán, that has traveled over 200 km from its origins at the Camarinal Sill. Some 32 solitons are in the packet; however, it is possible that these are actually two wave groups, with the higher-velocity leading waves of one packet overrunning the lower-velocity waves at the rear of the preceding group. At an average speed of 1 m/s, the implied age of this packet is approximately 2.3 days. Waves near the southern edge of the image seem to be refractively oriented along the shoals there. The ultimate eastern extent of the solitons in the Mediterranean has not been determined.

Figure 10 is an astronaut photograph taken from the Space Shuttle on 11 October 1984 (12:21:48 GMT). The photo contains three packets of internal solitons, each separated by approximately 30 km. The photograph shows several ubiquitous features of the internal waves: (a) alternate

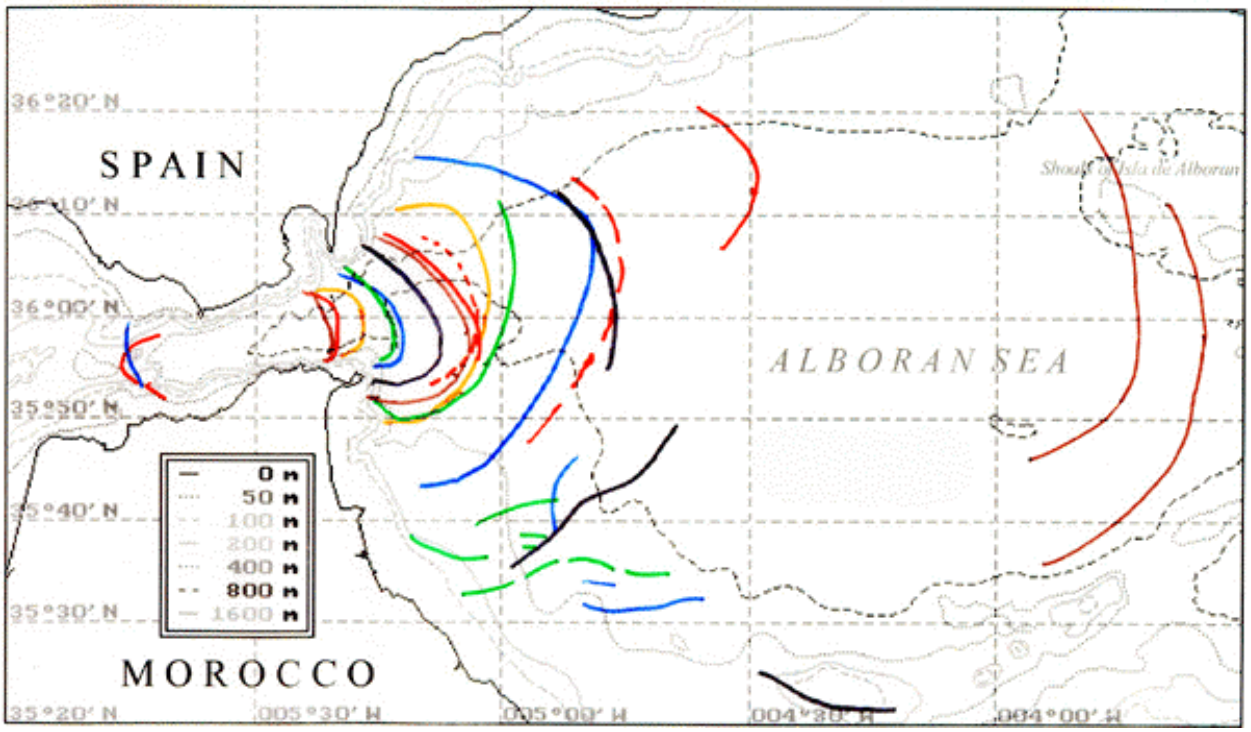

Figure 11. Map summarizing leading waves in soliton packets observed in ERS-1/2 imagery (solid lines) and in Shuttle photos (dashed lines). The Northeast and Southeast modes are visible.

packets tend to be weaker/stronger; (b) alternate packets drift toward the northeast or the southeast; (c) wavelengths and packet dimensions increase as time and space go on.

A total of 38 ERS images of the area collected between 1994 and 1997 were analyzed. All were nighttime images taken near 22:30 UTC. Twenty-one images had some internal wave signature(s) of interest. Of these, 13 displayed pulses of solitons radiating into the Alboran Sea at various distances from their source at the Camarinal Sill. Since the satellite is usually in an exact repeat orbit, viewing the same area on integral multiples, $n\tau$ (τ = 24 h, n = 35 days), the diurnal tide period of about 25 hours will be surveyed at one hour earlier on each repeated overpass. Mixed into these (badly aliased) observations are fortnightly, seasonal, and semiannual changes, all of which contribute variability to the solitons. It is known from several sets of observations made elsewhere that the fortnightly tidal forcing is important [Apel et. al, 1985; Liu et. al, 1985]. Usually if there are solitons generated, they will appear near the peak spring tide flows in the 14-day interval but will be absent at the neap tides. The observed ratio of soliton-containing images to total is 21/38 = 55%, which is about what is expected as an average over the fortnightly period.

The data from the ERS-1/2 (solid lines) and Shuttle (dashed lines) missions are summarized in Figure 11. The positions of the leading oscillation in each pulse are plotted on the bathymetric chart derived from GEBCO data [IOC, 1997]. The chart thus displays the propagation of solitons into the Mediterranean Sea, albeit over a wide variety of times. The pulse fronts in this representation are not, of course, as might be seen at one-hour intervals, but the evolution in

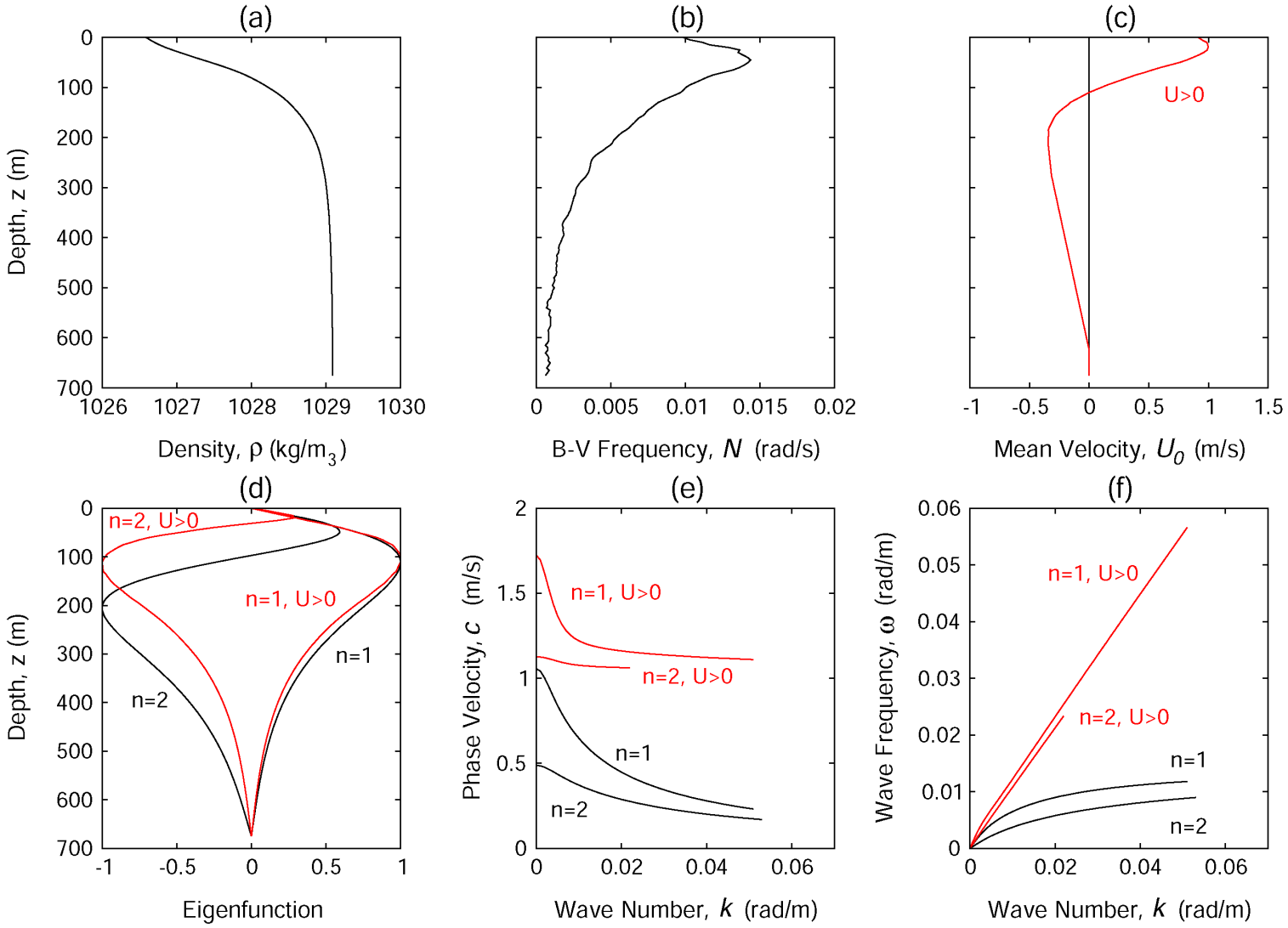

Figure 12. a) Typical undisturbed Density Profile for Gibraltar b) derived Brunt-Väisälä frequency $N(z)$ c) current flow profile d) Normalized vertical eigenfunctions (mode 1 & 2) for $2\pi/k_0$ = 900 m, H = 675 m for density and velocity profiles shown e) Phase Velocity f) Dispersion relations. The red curves show the effect of current (U > 0).

space *is* displayed. Internal waves are refracted by a combination of pycnocline and total water depths, and when their wavelengths (which are near 1000–2000 m) become of the order of the depth, refraction acts strongly. In addition, wave phase speeds are 1–2 m/s and thus solitons can be advected and distorted by tidal and coastal currents. All these processes govern the wavefront shapes.

KDV Parameters

Figure 12 shows a typical undisturbed density profile for the Strait of Gibraltar (Cournelle, personal communication, 1999). The normalized Mode 1 and Mode 2 eignefunctions have been evaluated for $l = \frac{2}{pk_0} = 900m$, with H = 675 m. For long waves ($k \to 0$) the maximum first mode wave speed (c_0) is computed to be 1.05 m/s without the effect of current shear (1.72 with current shear). Figures 12e and 12f give the phase velocity and dispersion relations for the data. The red curves include the effect of current. Table 3 presents the environmental coefficients and KDV parameters evaluated at k_0 for both the $U_0 = 0$ and $U_0 > 0$ cases.

Table 3. Environmental Coefficients and KDV parameters (λ_0=900) Gibraltar Solitons (without Current)

Long Wave Speed c_0 (m/s)	Nonlinear coefficient $1/\alpha$ (m)	Dispersion Factor $\gamma^{1/2}$ (m)	Amplitude (KDV theory) h_0 (m)	Non-Linear Phase Velocity V (m/s) for (s^2=1)
1.05	-62.1	78.4	-27.89.	1.36

Environmental Coefficients and KDV parameters (λ_0=900) Gibraltar Solitons (with Current)

Long Wave Speed c_0 (m/s)	Nonlinear coefficient $1/\alpha$ (m)	Dispersion Factor $\gamma^{1/2}$ (m)	Amplitude (KDV theory) h_0 (m)	Non-Linear Phase Velocity V (m/s) for (s^2=1)
1.72	-74.62	46.60	-11.85	1.90

Westward Propagating Internal Waves

Figure 13 shows an example of a westward propagating soliton approximately 30 km west of the Camarinal Sill and at its western neighbor, the Spartel Sill. The comprehensive studies by [Armi and Farmer 1985, Armi and Farmer 1988] contain a report of the existence of internal waves in the region of the two sills. The images thus provide proof that for this strategic strait, at least, the soliton generation process is bilateral but not bisymmetric. These westward waves are smaller in wavelength than those waves radiating into the Mediterranean and do not appear as often in the imagery. Brandt et al. [1996] interpreted the westward waves as being associated with the seasonal thermocline present in the region during summer and not the halocline between the Atlantic and Mediterranean waters.

North and South Propagating Internal Waves

While the most prominent internal waves are those generated at the Camarinal Sill and propagate eastward, shore based radar observations carried out in 1986 [Watson and Robertson 1990] detected northward travelling internal waves (toward Gibraltar) during the spring tide. The

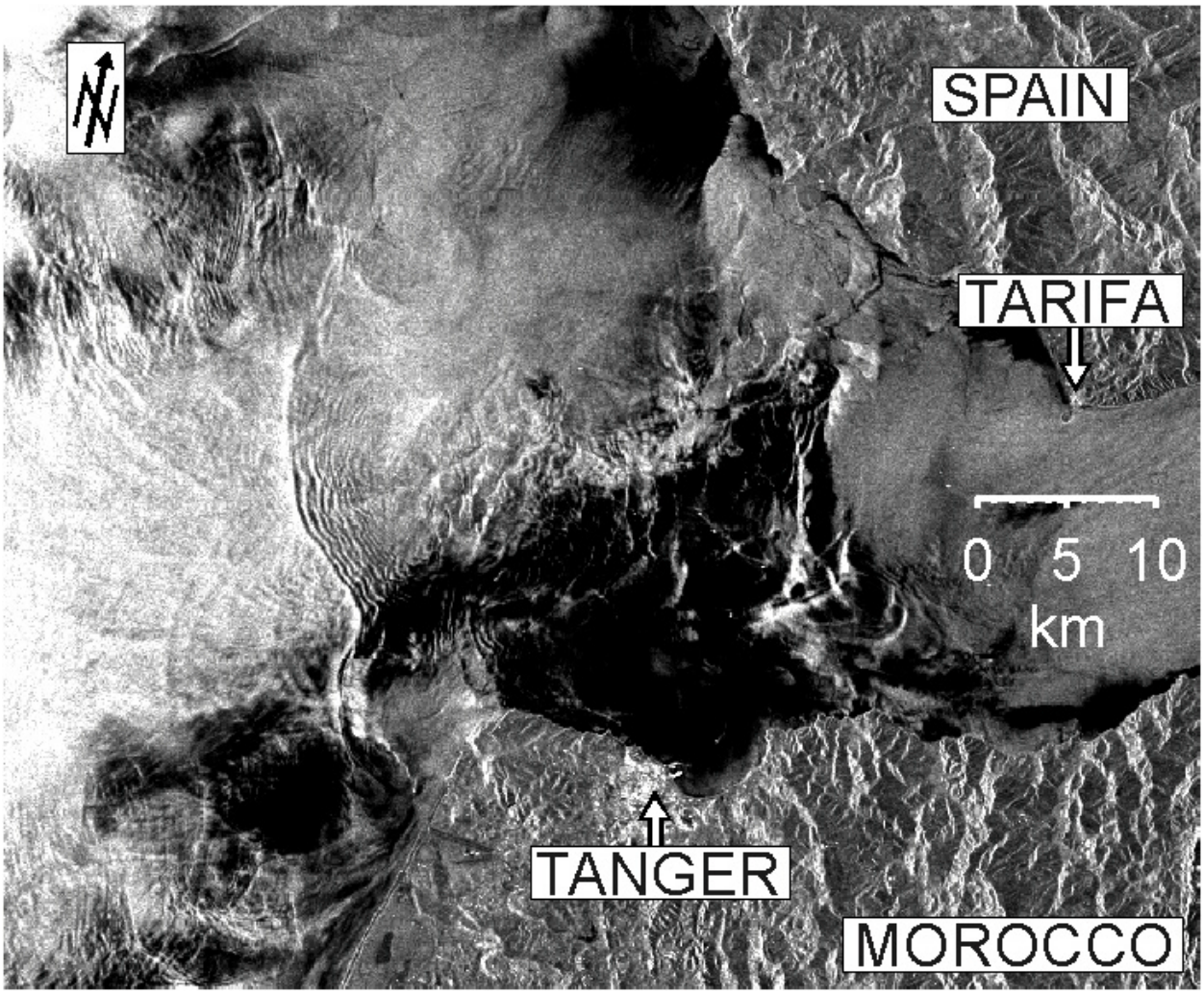

Figure 13. ERS-1 SAR image of the Strait of Gibraltar acquired on Aug. 5, 1994, at 2241 UTC, 3 h 8 min after low tide at Tarifa. It shows sea surface manifestations of an internal wave train propagating out of the Strait of Gibraltar towards the Atlantic Ocean. Note the small wavelength in this wave train as compared to the wavelength in wave trains propagating into the Mediterranean Sea. Probably, this internal wave train is linked to a seasonal thermocline. [Image from Alpers et al. 1996. Image courtesy of Werner Alpers]

existence of the waves was confirmed by Alpers and La Violette [1992] using ERS-1 SAR data who also identified corresponding southward propagating waves towards Ceuta. [ERS-1 February 21, 1992 11:03 UTC (orbit 3574, frames 2871 and 2889) and March 22, 1992 at 11:03 UTC (orbit 3574, frames 2871, and 2889)]. Watson and Robertson [1990] found no correlation between the arrival times of the northward waves and the main eastward wave and no satisfactory explanation of the waves origin yet exist. Watson and Robertson hypothesize the waves have a bathymetric origin and gain amplitude as shock waves in the supercritical flow. The waves propagate as the tide turns and the flow decreases [Alpers and La Violette 1992]. Figure 14 is an ASTER image from July 2000. The image shows a northward propagating internal wave in the presence of an eastward internal wave packet. Figure 15 is an ERS-2 image of the western end of the strait taken on 4 February 2002. The image appears to show a strong northward propagating wave approaching Tarifa. A similar wave is also visible in figure 13

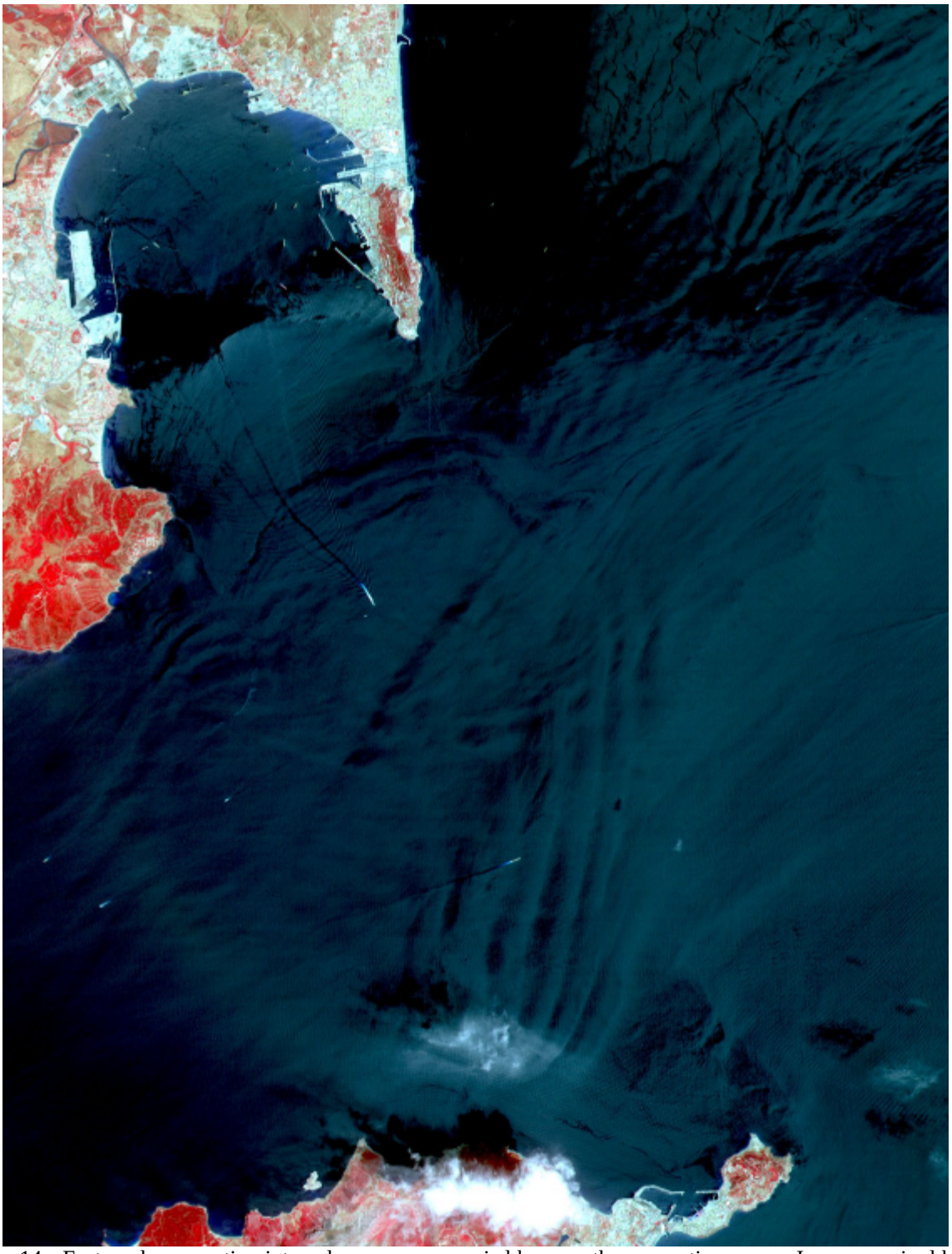

Figure 14 - Eastward propagating internal wave accompanied by a north-propagating wave. Image acquired by the Advanced Spaceborne Thermal Emission and Reflection Radiometer (ASTER) on July 5, 2000. Image dimension 25 x 33.5 km. Image courtesy JPL Catalog #: PIA02657.

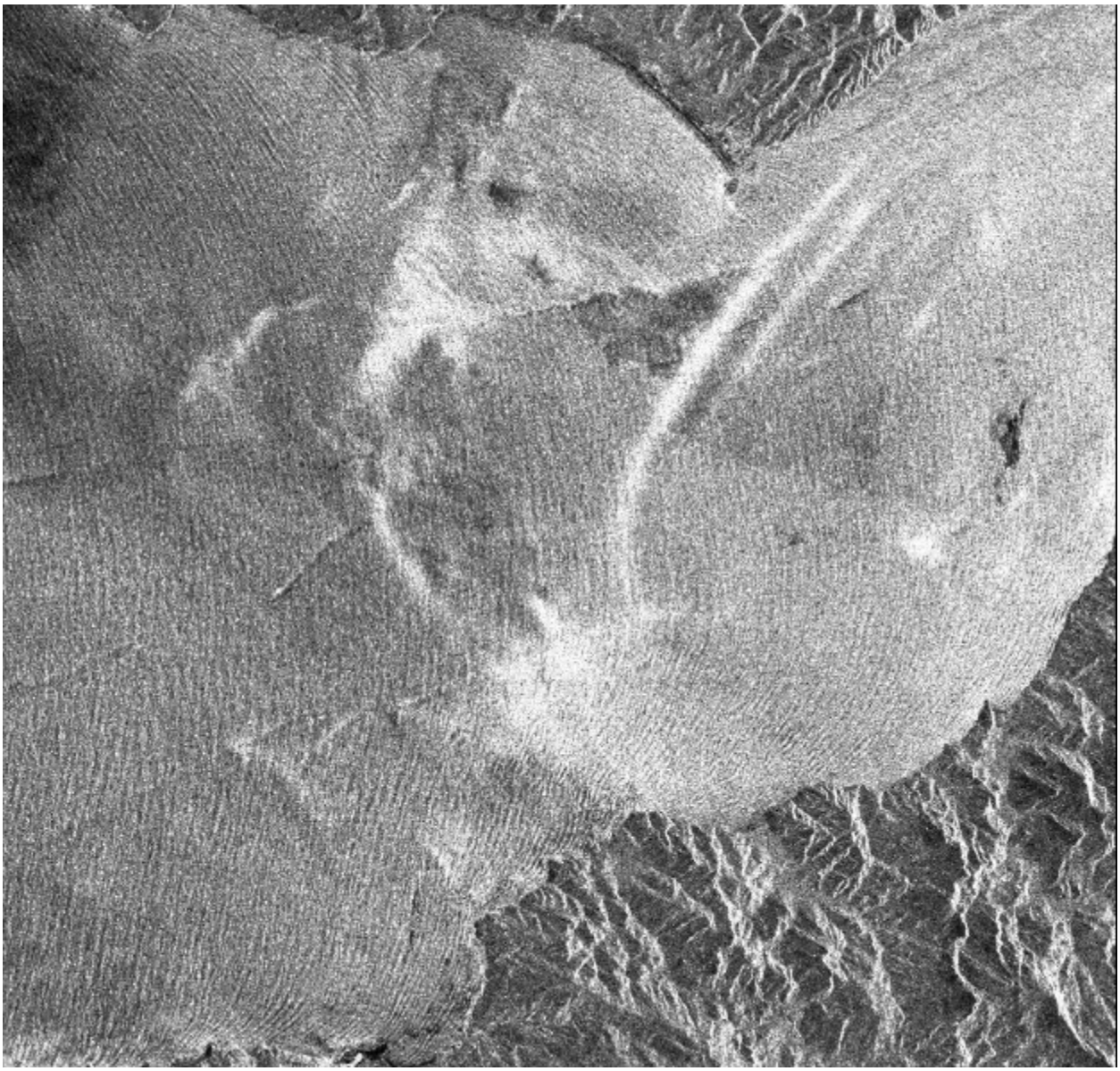

Figure 15 ERS-2 Image of the western part oaf the Strait of Gibraltar (Orbit 35519 Frame 2885 4 February 2002 11:3:41 GMT). Image dimension 50 km x 50 km. Tarifa is located on the point in the upper center of the image. [Image ESA ©2002 from http://earth.esa.int/ers/ers_action]

Camarinal Sill - Roughness Patterns

The fourth feature that repeatedly appears on imagery from the Gibraltar area is a quasi-stationary roughness pattern observed over the Camarinal Sill. The feature is shown in Figures 16 and 17 and also appears in figures 10 and 15. La Violette and Arnone [1988] report that the distinct roughnes pattern is almost always present over the Camarinal Sill, with exception of low tide. Brandt et al. [1996] interprets the patterns as quasi-stationary depressions of the interface in the region. Figure 16 shows how the pattern changes position with tidal flow variation. Figure 17 shows a roughness pattern over the Camarinal Sill taken from helicopter in 1984. La Violette and Arnone [1988] reports that ships during this period of observation leaving the chop had lost their heading.

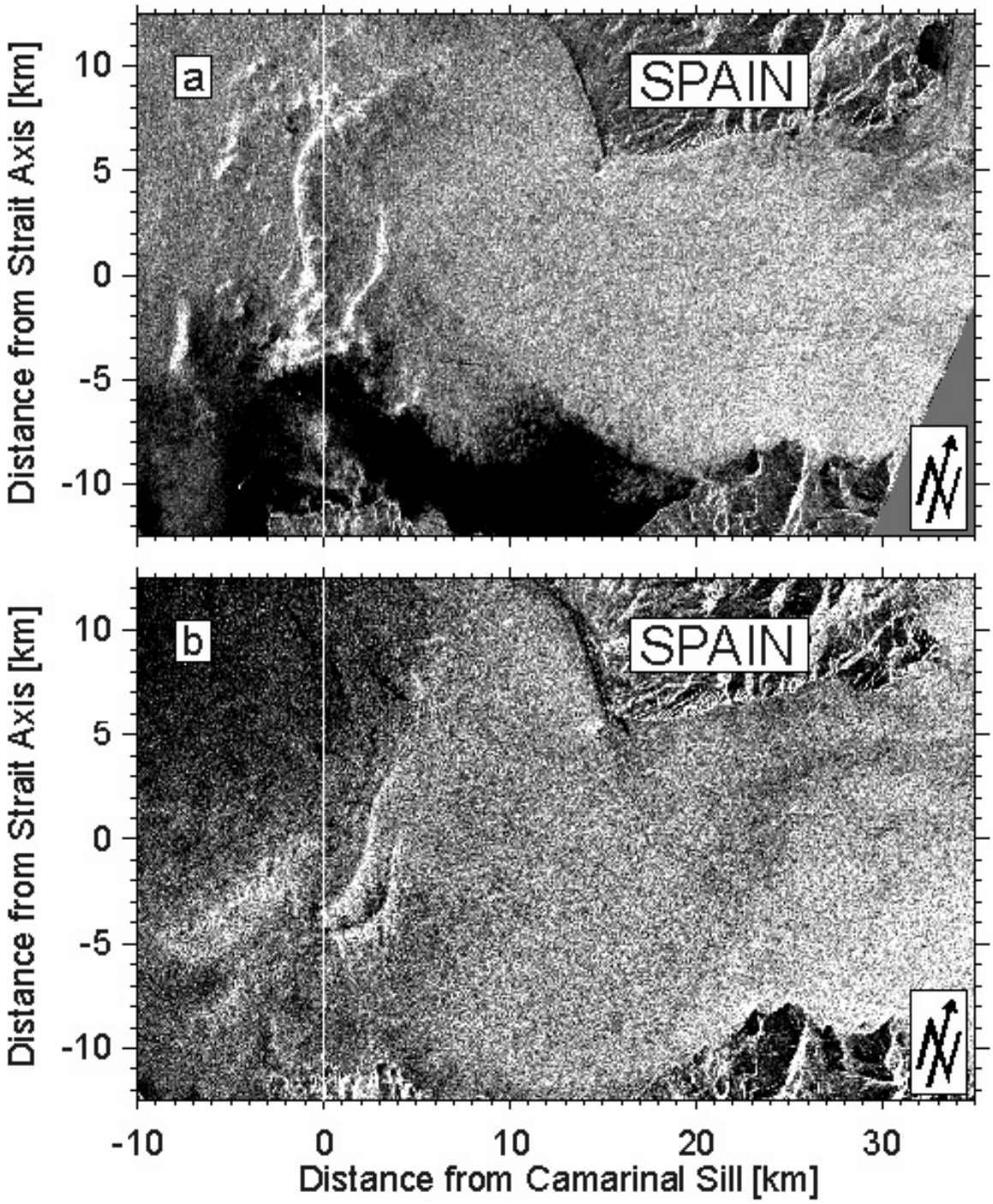

Figure 16 Two ERS-1 SAR images of the Strait of Gibraltar including the Camarinal Sill acquired at different phases of the tidal cycle: (a) 2 h 47 min after low tide at Tarifa (Jan. 08, 1993, 1105 UTC); (b) 5 h 31 min after low tide at Tarifa (Jan. 08, 1994, 1103 UTC). The upper image (a) was acquired approximately at maximum westward tidal flow and the lower image (b) approximately at slack water after maximum westward tidal flow. The images show bright lines near the Camarinal Sill, which are sea surface manifestations of strong depressions of the halocline. [Image from Alpers et al. 1996 and Brandt et al. 1996. Image courtesy of Peter Brandt]

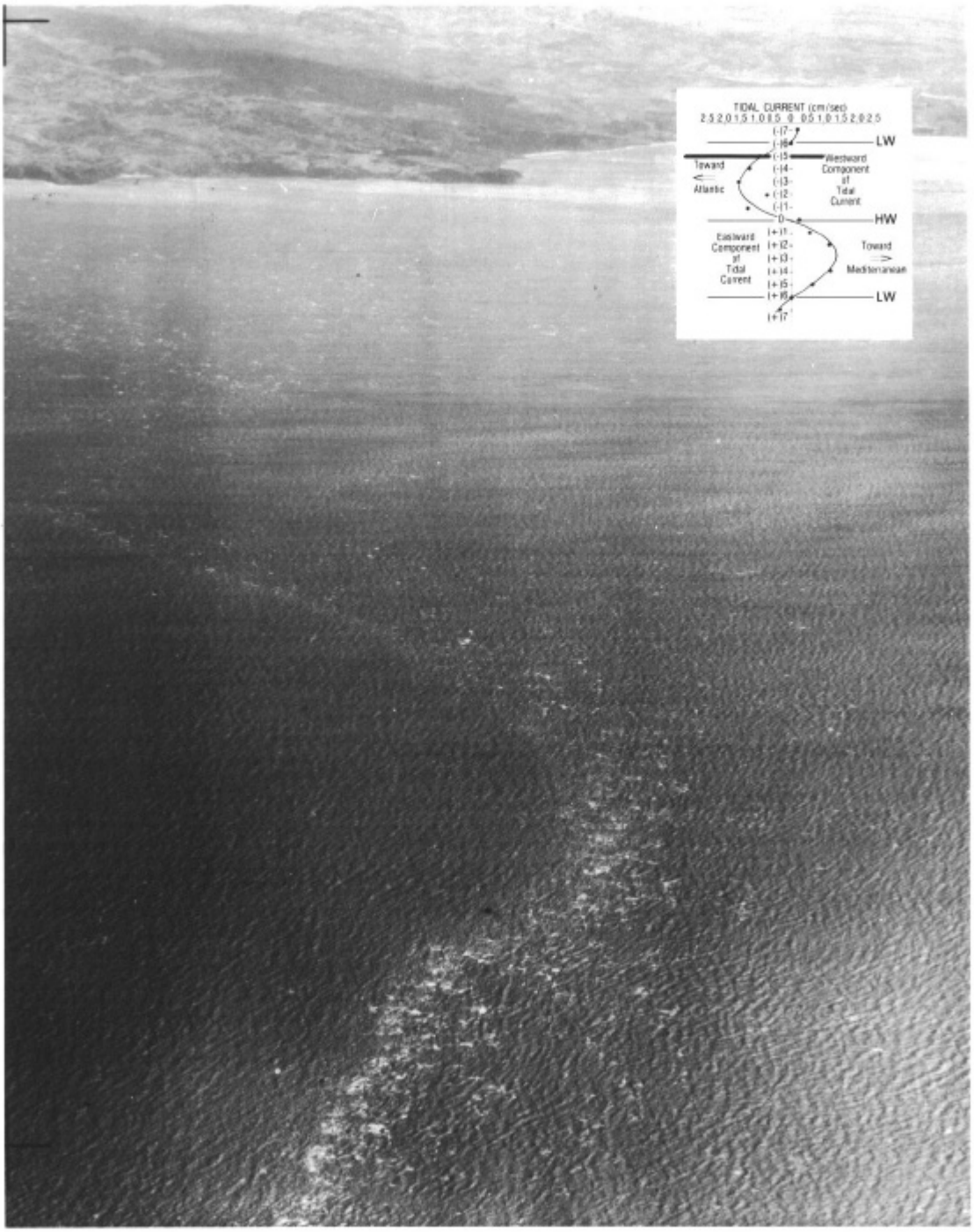

Figure 17. Surface roughness pattern over the Camarinal Sill on 11 October 1984 at 0830 GMT (-4 HW) Photography taken from a helicopter at an altitude of 700 m looking south toward the Gulf of Tangiers. [From La Violette and Arnone 1988]

References

Alpers, W., P. Brandt, A. Rubino, and J.O. Backhaus: (1996) "Recent contributions of remote sensing to the study of internal waves in the Straits of Gibraltar and Messina", in: Dynamics of Mediterranean straits and channels, F. Briand ed., CIESM Science Series no.2, Bulletin de l'Institut Océanographique, Monaco, no. spécial 17, 21-40.

Alpers, W., and P. E. La Violette: (1993) "Tide-generated nonlinear internal wave packets in the Strait of Gibraltar observed by the synthetic aperture radar aboard the ERS-1 satellite", Proceedings of the First ERS-1 Symposium - Space at the Service of our Environment, held at Cannes, France, November 4-6, 1992, published by ESA, Paris, France, ESA SP-359 (March 93), 753-758, 1993.

Apel, J. R. and P. F. Worcester, 2000: "Internal solitons near Gibraltar: A longitudinal study using ERS-1 and 2 SAR imagery," in Proc. ERS–Envisat Symposium: Looking Down to Earth in the New Millennium, European Space Agency, ESRIN/Publications.

Apel, J. R., 2000, "Solitons near Gibraltar: Views from the European Remote Sensing Satellites," Report GOA 2000-1, Global Ocean Associates, Silver Spring, MD. 23 pp.

Apel,J.R., J.R.Holbrook, J.Tsai,and A.K.Liu,1985,"TheSuluSeainternal soliton experiment," J. Phys. Oceanogr., 15 (12), 1625-1651.

Armi, L. and Farmer, D. (1985) The internal hydraulics of the Strait of Gibraltar and associated sills land narrows, Oceanologica Acta 8, 37-46.

Armi, L., and D.M. Farmer, (1988) The flow of Mediterranean water through the Strait of Gibraltar, Prog. Oceanogr., 21, 1-105.

Boyce, F.M., (1975) Internal waves in the Straits of Gibraltar, Deep Sea Res., 22, 597-610.

Brandt, P., W. Alpers, and J.O. Backhaus: (1996) "Study of the generation and propagation of internal waves in the Strait of Gibraltar using a numerical model and synthetic aperture radar images of the European ERS 1 satellite", J. Geophys. Res., 101, 14,237-14,252.

Bray, et al, (1990) Generation and kinematics of the internal tide in the Strait of Gibraltar, in The Physical Oceanography of Sea Straits, edited by L.J. Pratt, pp. 477-491, Kluwer Acad., Norwell, Mass.

Farmer, D.M., L. Armi, (1988) The flow of Mediterranean water through the Strait of Gibraltar, Prog. Oceanogr., 21, 1-105.

Frassetto, R., (1960) A preliminary survey of thermal microstructure in the Strait of Gibraltar, Deep Sea Res., 7, 152-162.

IOC, IHO, and BODC, "GEBCO-97: The 1997 edition of the GEBCO digital atlas," British Oceanographic Data Centre, National Environmental Research Council, Birkenhead, U.K. 1997

Kinder, T.H., and G.K. Bryden, (1987) The 1985-1986 Gibraltar Experiment: Data collection and preliminary results, Eos Trans. AGU, 68, 786-787, 793-795.

Lacombe, H and C. Richez (1982) The regime of the Strait of Gibraltar, in Hydrodynamics of Semienclosed Seas, J.C.J Nihoul, ed., pp. 13-73, Elsevier, New York.

Lacombe, H. and C. Richez, (1984) Hydrography and currents in the Strait of Gibraltar. Sea Straits Research Atlas SSR-3, National Ocean Research and Development Activity, NSTL, Mississippi 39529.

La Violette, et al, (1986) Measurements of internal waves in the Strait of Gibraltar using a shore-based radar, Tech. Rep. 118, 13 pp., Nav. Ocean Res. and Develop. Activ., Natl. Space Technol. Lab., Bay St. Louis, Miss.

Liu, A.K., J.R. Holbrook, and J.R. Apel, 1985, "Nonlinear internal wave evolution in the Sulu Sea," J. Phys. Oceanogr.15 (12), 1613-1624.

Pettigrew, N.R. and R.A. Hyde, (1990) The structure of the internal bore in the Strait of Gibraltar and its incluence on the Atlantic inflow, in the Physical Oceanography of Sea Straits, edited by L.J. Pratt, pp. 493-508, Kluwer Acad., Norwell, Mass.

Richez, C., (1994) Airborne synthetic aperture radar tracking of internal waves in the Strait of Gibraltar, Prog. Oceanogr., 33, 93-159.

Watson, G., and I.S. Robinson, (1990) A study of internal wave propogation in the Strait of Gibtraltar using shore-based marine radar images, J. Phys. Oceanogr., 20, 374-398.

Zeigenbein, J., (1969) Short internal waves in the Strait of Gibraltar, Deep Sea Res., 16, 479-487.